

Chapter 5

Theoretical Considerations

The theoretical notions described in this chapter are used to describe the experiments performed throughout this work. An introductory description of wave packets, their generation and propagation is given. The detection of wave packet motion in real time by means of femtosecond pump-probe spectroscopy together with a few typical examples is presented as well. The last section treats the present used methods of controlling molecular processes by employing femtosecond pulses. Special attention is devoted to the optimal control method, in particular adaptive feedback control, used to influence chemical reactions with shaped laser pulses.

5.1 Molecular Dynamics – A Short Introduction

5.1.1 Wave Packets

The time-dependent Schrödinger equation describes the dynamics of an isolated molecule in a potential $V(\mathbf{r})$ is [65]:

$$i\hbar\frac{\partial}{\partial t}\psi(\mathbf{r}, t) = H\psi(\mathbf{r}, t). \quad (5.1)$$

where the Hamilton operator in the absence of an external field is

$$H = -\frac{\hbar^2}{2m}\nabla^2 + V(\mathbf{r}) \quad (5.2)$$

Note that the Hamilton operator does not explicitly depend on time. The solutions of the time-dependent Schrödinger equation are [65]:

$$\psi(\mathbf{r}, t) = \sum_{j=1}^{\infty} c_j \psi_j(\mathbf{r}) e^{-\frac{i}{\hbar} E_j t}. \quad (5.3)$$

The equation (5.3) describes a *wave packet*, a linear superposition of the eigenstates $\psi_j(\mathbf{r})$. $\psi(\mathbf{r}, t)$ is time-dependent, meaning that the superposition of states can evolve in time. The time-independent states $\psi_j(\mathbf{r})$ are solutions of the time-independent Schrödinger equation $H\psi_j(\mathbf{r}) = E_j\psi_j(\mathbf{r})$ with the eigenvalues E_j .

Taking into account that the probability density is determined by

$$|\psi(\mathbf{r}, t)|^2 = \sum_{j,k=1}^{\infty} c_k^* c_j \psi_k^*(\mathbf{r}) \psi_j(\mathbf{r}) e^{-\frac{i}{\hbar} (E_j - E_k) t}. \quad (5.4)$$

the following statement can be made: the probability density is time dependent if there are at least two energy levels. The temporal evolution of the wave packet represents then the periodical modification of the location probability, with a frequency corresponding to the energy difference $E_j - E_k$ of the two participating levels.

5.1.2 Laser–Molecule Interaction

The laser field induces a perturbation in the molecular system. Thus the total Hamiltonian operator has the form $H_{tot} = H + H'$, where H is the molecular hamiltonian from the equation (5.1). $H' = -\mathbf{D} \cdot \mathbf{E}$ describes the perturbation induced by the laser field, which couples to the molecule by the dipole moment operator \mathbf{D} . The dipole approximation (for weak laser fields) gives the time dependence between the laser light and the molecule $V = -\mu \cdot E(t)$, whereby μ is the component of the dipole operator parallel to the electric field. Here the electric field is treated for simplicity reasons as one-dimensional.

In the case of a transition between two electronic states ψ_1 and ψ_2 the time-dependent Schrödinger equation can be written as follows [66]:

$$i\hbar \frac{\partial}{\partial t} \begin{pmatrix} \psi_1(t) \\ \psi_2(t) \end{pmatrix} = \begin{pmatrix} H_1 & -\mu_{12} E^*(t) \\ -\mu_{21} E(t) & H_2 \end{pmatrix} \begin{pmatrix} \psi_1(t) \\ \psi_2(t) \end{pmatrix}$$

In the frame of Born-Oppenheimer approximation, the Hamiltonians H_1 and H_2 contain a kinetic energy term and a potential energy term and they govern the dynamics on the electronic states 1 and 2. The potential energy term describes the Coulomb interaction between electrons and nuclei, as well as

the electron-electron and nuclei-nuclei interactions which is different for each of the two states.

The additional term H' describes a transition between the electronic states 1 and 2 by absorbing one photon if

$$\langle \psi_1 | \mu_{12} \cdot E | \psi_2 \rangle \approx \langle \psi_1 | \mu_{12} | \psi_2 \rangle E \neq 0 \quad (5.5)$$

because the electric field is assumed to be homogeneous over the molecule.

The transition dipole moment is

$$M = \langle \psi_1 | \mu_{12}(x, X) | \psi_2 \rangle \quad (5.6)$$

where x is the one-dimensional electron coordinate and X is the one-dimensional nuclear coordinate. It is common to neglect the rotational motion since its inclusion does not change the result. Hence the wave functions consist of an electronic part and a vibrational part: $\psi_i = \psi_{e,i} \psi_{vib,i}$ for $i = 1, 2$. Consider that the initial state is a vibrational eigenstate described by \hat{H}_1 , i.e. $\hat{H}_1 \psi_{e,1} = E_1 \psi_{e,1}$; thus no dynamics occurs in the first state. Then the transition dipole moment can be written

$$M = \langle \psi_{e,1} \psi_{vib,1} | \mu_e(x) | \psi_{e,2} \psi_{vib,2} \rangle + \langle \psi_{e,1} \psi_{vib,1} | \mu_N(X) | \psi_{e,2} \psi_{vib,2} \rangle \quad (5.7)$$

where the first term describes the electronic excitation. It can be shown that the second term is zero, since the electronic wave functions of two different states are orthogonal. Therefore the transition dipole moment has the following form:

$$M = \langle \psi_{e,1} | \mu_e(x) | \psi_{e,2} \rangle \cdot \langle \psi_{vib,1} | \psi_{vib,2} \rangle \quad (5.8)$$

Hereby the first term is the electronic transition dipole moment and the second is known as vibrational overlap integral whose square is called Franck-Condon factor. The vibrational overlap integral can be separated from the rest of the integral in equation (5.8) based on the Franck-Condon principle. The Franck-Condon principle states that the time in which a transition occurs between vibrational states is so short ($< 10^{-15}$ s) compared to the vibrational period of the molecule, that the nuclear configuration remains unchanged during the transition. Thus transitions occur vertically and the kinetic energy of the molecule is the same immediately before and after the electronic transition. In a classical picture, the wave packet spends more time at the inner and outer turning points of the potential well of the electronic state than in the middle. Thus the electronic transitions occur at the outer or inner turning points where the wave packet is most localized [67].

5.1.3 Generation of Wave Packets

Although in the beginning the preparation of wave packets seemed almost impossible, the advent of femtosecond lasers allowed their generation (and observation), because the duration of the femtosecond pulse is much shorter than the typical duration of molecular dynamics.

A method to generate a wave packet is to apply a short, particularly a femtosecond, pulse to a molecule in its equilibrium state. Usually this is the ground state ($v = 0$), where the wave packet is stationary and relatively narrow. Molecules in their vibrational ground state ($v = 0$), can be generated in a cold molecular beam (see Chapter 4). The laser pulse transfers the wave packet onto a particular excited state potential surface which is not in equilibrium. Thereby the resonance condition between the two electronic states is satisfied by the central laser wavelength and the spectral bandwidth.

5.1.4 Monitoring Wave Packet Dynamics in Real-Time

The most widely used technique to monitor time-dependent wave packet motion is the *pump-probe* spectroscopic scheme. In its simplest form, the pump-probe technique can be outlined as follows (see also Figure 5.1).

- **Pump.** A first short laser pulse prepares a wave packet in a non-stationary state, wherefrom the system can evolve. This corresponds to zero on the measured time scale (when the femtosecond clock starts to tick).
- **Probe.** A second short pulse is used to send the molecular system in a detectable state. This occurs after a defined, but variable delay time Δt . The measured signal can be ion current, fluorescence, photoelectron current, etc.
- **Delay.** This delay time is varied so that the signal is recorded as a function of time (molecular motion picture). Certainly one expects a time-dependent signal, since the wave packet is prepared in an intermediate nonstationary state.

Since the potential surfaces of the electronic states involved in an electronic transition depend on the reaction coordinate, a resonant excitation produced by the pump pulse takes place only in certain spatial regions. This is also known as the Franck-Condon window which has a maximum at those positions where the potential difference $V_2 - V_1$ equals the laser frequency. The Franck-Condon window of excitation is limited by the Franck-Condon

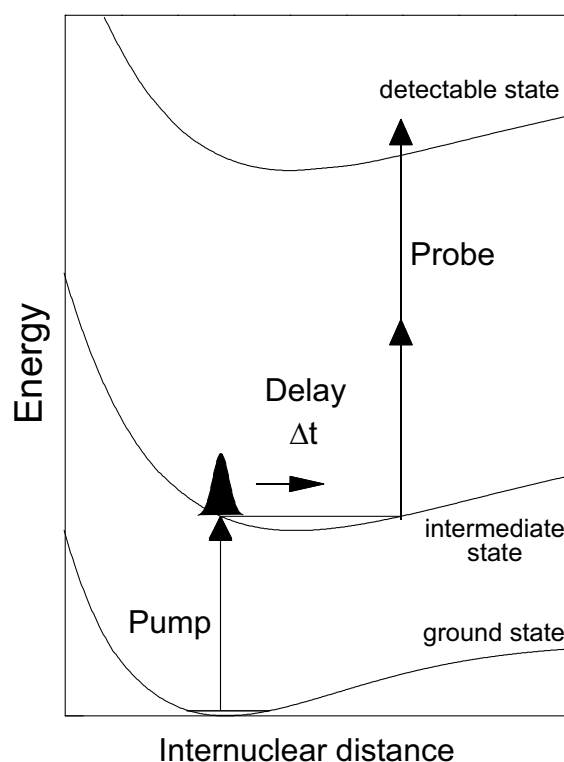


Figure 5.1: Principle of fs pump–probe experiments. The pump pulse generated a wave packet in the state of interest. The probe pulse monitors in real time the wave packet position on this state as a function of delay time Δt as long as the population in the detectable state is a function of the nuclear coordinate.

factors. Similarly, there is a Franck-Condon window for the probe process, when the wave packet is transferred to the detectable state.

Typically, the initial state is the ground state of the molecule, the non-stationary state corresponds to an intermediate excited state which is to be examined. Detectable states can be excited states in the neutral, whereby their population is measured by fluorescence [68] or absorption of probe photons [69]. Stimulated emission caused by the probe pulse can be also measured if the detectable state is energetically lower [70].

The ionic state is commonly taken as detectable state in many fs pump–probe experiments [71, 72]. Thereby Two-Photon Ionization (TPI) spectroscopy in time domain is employed. The molecules are electronically excited by the first laser of energy $\hbar\omega_1$ from the electronic ground state. The second laser of energy $\hbar\omega_2$ ionizes the particles. In a pump–probe experiment the energy of the first laser $\hbar\omega_1$ is no longer tuned to record the ion yield

as a function of laser energy; the ion current is now measured as a function of the time delay between the two laser fields. If more photons are involved in the ionization process the technique is known as Multi-Photon Ionization (MPI). However if a resonant transition via an electronic state takes place in the ionization process the technique is commonly called Resonant-Enhanced Multi-Photon Ionization (REMPI). The latter method is used in this work.

In order to investigate wave packet dynamics in the ground state, the recently developed NeNePo (Negative-to Neutral-to Positive) scheme is most appropriate [73]. Hereby the experiment starts with a negative molecule which loses an electron after interaction with the pump pulse (photo-detachment), whereby a wave packet is generated in the ground state of the neutral species. Its ground state motion is recorded by the probe pulse by multi-photon ionization. A detailed overview of applied pump-probe technique and its variations can be found in Refs. [12, 14].

Wave packet dynamics were observed in many femtosecond pump-probe experiments. *Femtosecond clocking of a chemical bond* is now a popular expression. Zewail and co-workers have observed for the first time the bond-breaking in the ICN molecule by using fs laser pulses [3]. The wave packet was prepared on a dissociative surface by the pump pulse. The second pulse transfers the population on a second excited state, which is also a dissociative one. The frequency of the absorbed laser light gives information about the separation of the two potential energy surfaces (PES) and therefore about the position of the outgoing wave packet.

Figure 5.2 displays possible situations of wave packet dynamics which can be investigated by means of femtosecond pump-probe spectroscopy. The following cases are described below:

- A.** Bound-bound transition (Figure 5.2a). The wave packet is prepared in a bound-bound state by the pump pulse at the inner turning point of the excited state potential well and it oscillates between the inner and the outer turning point of this potential well. Depending on the time when the probe pulse arrives one is able to observe this vibrational motion if the ionization probability is a function of the reaction coordinate. A typical example is given in Figure 5.2d for the NaK dimer. The wave packet motion is detected in a 3-photon ionization process (spectrum reproduced after Ref. [74]).
- B.** Bound-free transition (Figure 5.2b). The wave packet is generated on a repulsive state. The cluster dissociates directly and the pump-probe spectrum consists of a broad featureless peak. The exponential decay reflects the lifetime of the investigated cluster on the electronic

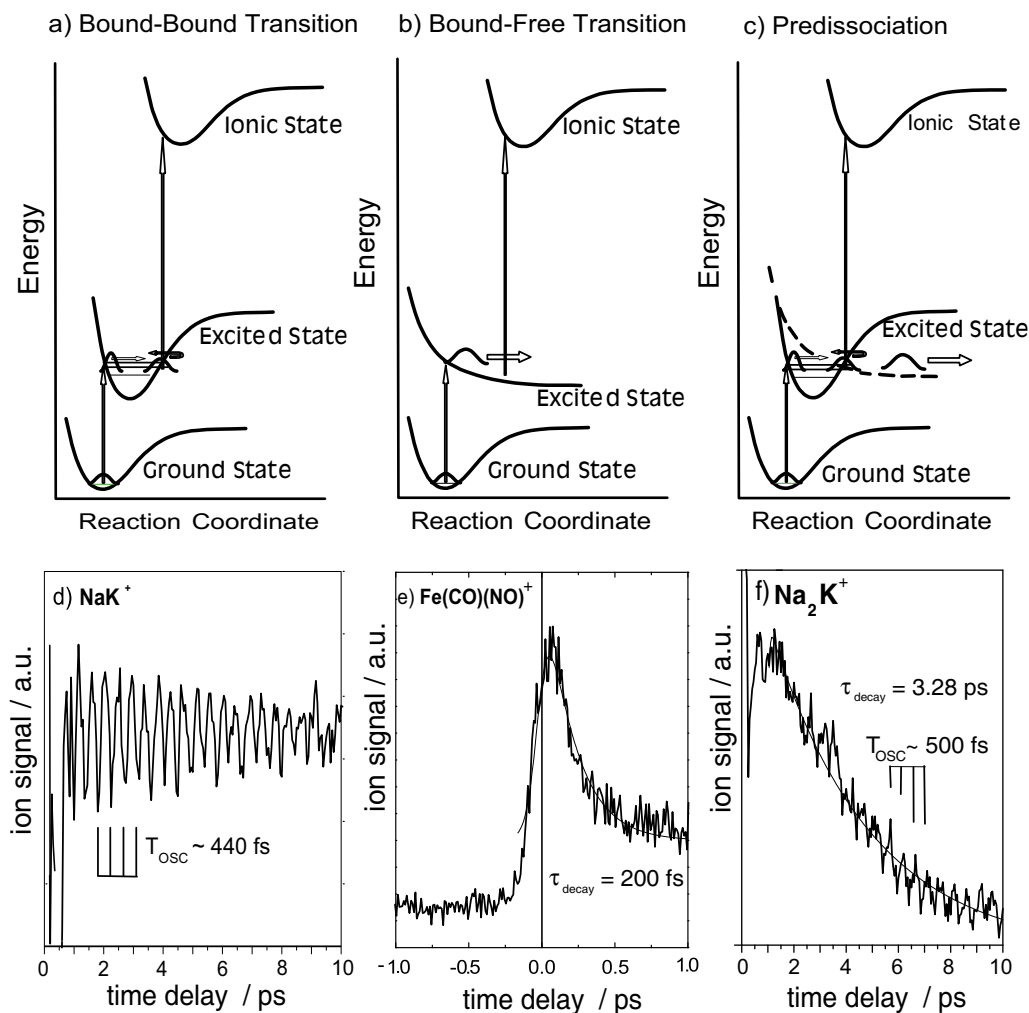


Figure 5.2: Scheme of different fs pump-probe experiments. a) Excited state wave packet dynamics of a bound-bound transition. One expects to measure wave packet oscillations, followed by dephasing (eventually fractional or total revivals). b) The case of a bound-free transition. The wave packet leaks out on the repulsive state and the molecule dissociates. In the pump-probe spectrum one expects to see a broad, structureless peak. c) The predissociation case, when the excited state potential curve supports a metastable state. The cluster dissociates, but it may as well oscillate on its way to fragmentation. Portions of the wave packet leak out on the dissociation channels every time it arrives at the crossing point. The pump-probe spectrum reveals a vibrational structure superimposed on an exponential decay.

excited state. This can be observed for the organometallic complex $\text{Fe}(\text{CO})(\text{NO})$, which fragments without any vibrational characteristic, as depicted in Figure 5.2e [59].

- C. Predissociative case (Figure 5.2c). The pump pulse creates a wave packet in an electronic excited state. Due to the coupling between the bound-bound and bound free state a portion of the wave packet can leak out into the dissociative channel. The probe pulse monitors the population on the bound-bound state. The pump-probe spectrum is expected to reveal oscillatory component superimposed on an exponential decay. The latter indicates the lifetime of the excited molecule. This is shown in Figure 5.2f for the Na_2K trimer, where oscillations of 500 fs period overlaid on exponential decay time of 3.28 ps can be observed [59, 75].

It is important to mention that the measured transient signals presented in this work represent the convolution of the population created on a particular electronic (e.g. excited) state with the response of the measured system, which is mainly due to the pulse duration. Usually, the response of the measured system is the cross-correlation function of the pump and probe pulses (in particular auto-correlation for one-color pump-probe experiments), assuming that they have a sech^2 shape. In order to quantitatively evaluate the measured kinetic traces and to extract the decay times from the experimental data, a deconvolution algorithm is necessary. In this way, the contribution of the laser pulses to the measured signal is excluded.

5.1.5 Femtosecond Pump-Probe Spectroscopy on K_2

The pump-probe experiments on the two potassium dimer isotopomers are displayed in Figure 5.3. These results were the starting point for the experiments presented in Chapter 9. The temporal evolution of the 3-photon ionization signal for the two species is recorded with femtosecond pulses centered around 833.7 nm. The observed dynamics reveal oscillations with a period of $T_{osc} \sim 500$ fs on the $\text{A}^1\Sigma_u^+$ electronic excited state (see also the potential energy curves in Figure 9.1). The time delay between the pump and probe pulse was varied between 0 and 200 ps.

In the pump-probe process, the wave packet is prepared in the $\text{A}^1\Sigma_u^+$ state. Due to selection rules, the $\text{b}^3\Pi_u$ state is dark during the femtosecond excitation [76]. The wave packet propagates along the $\text{A}^1\Sigma_u^+$ state, but the system can transfer to the $\text{b}^3\Pi_u$ state via spin-orbit coupling. The contribution of the $\text{b}^3\Pi_u$ state to the pump-probe is negligible since the resonant intermediate state $(2)^1\Pi_g$ is a singlet state. The first maximum in the spectrum

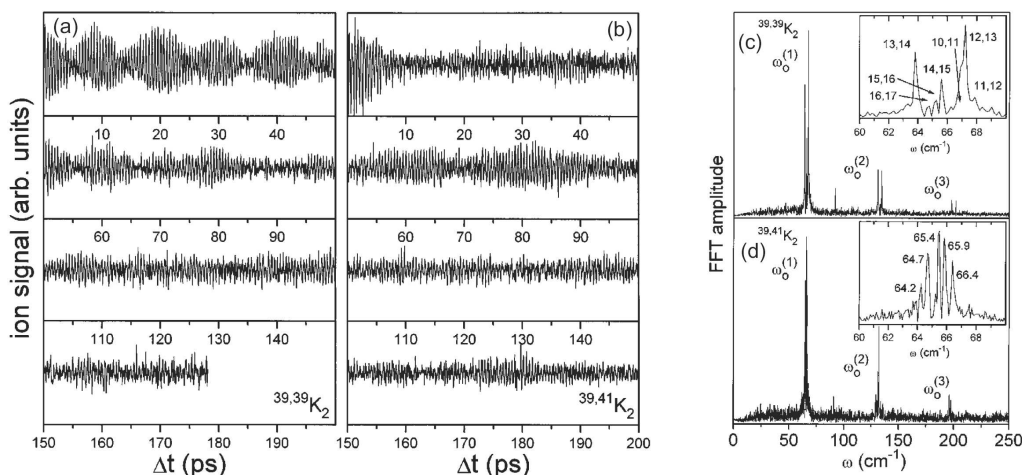


Figure 5.3: Time resolved spectra recorded for both isotopes $^{39,39}\text{K}_2$ (a) and $^{39,41}\text{K}_2$ (b). The spectra reveal the molecular dynamics in the $A^1\Sigma_u^+$ state. For the $^{39,39}\text{K}_2$ isotope a beating structure of the ion signal with a period of $T_{beat} \approx 10$ ps is observed, which denotes the total and fractional revivals of the wave packet. For $^{39,41}\text{K}_2$, the oscillatory behavior shows a regular dephasing of the wave packet with fractional revivals. Total revivals are observed at 38, 60 and 82 ps. The corresponding FFT analysis for the two isotopes is shown as well. The frequency group ω_0^1 for $^{39,39}\text{K}_2$ (c) contains two dominant frequencies, responsible for the beat structure. They are a consequence of the shifting of the vibrational levels due to the spin-orbit coupling. The FFT spectrum for $^{39,41}\text{K}_2$ (d) shows a typical anharmonic behavior of the frequency components [53].

from Figure 5.3a appears at 250 fs, indicating that the resonant ionization step performed by the probe pulse takes place at the outer turning point. The two isotopes show totally different behavior. The time-resolved spectrum of $^{39,39}\text{K}_2$ is dominated by a beating feature with a period of $T_{beat} = 10$ ps. The first maximum of the beat structure appears at 10 ps. With increasing propagation time, the wave packet dephases, the amplitude of the oscillations decreases, and the wave packet is not localized anymore. At times when the frequency components are again in phase, an oscillation pattern appears, similar to the one at the beginning of the real-time spectrum. This phenomenon is known as *wave packet revival* [77]. The time when the wave packet revival takes place is [77]

$$T_{rev} = 2T_{osc} \left(\hbar \frac{\partial \omega}{\partial E} \right)^{-1} \quad (5.9)$$

where T_{osc} is the classical oscillation period in the anharmonic potential $E(\omega)$.

Fractional revivals refers to the fact that the wave packet can split in several parts, due to dephasing, which may reappear at longer times. For example, fractional revivals were observed in the B-state of Br₂ [78] in the A¹Σ⁺ state of NaK [74] and in the A¹Σ_u⁺ state of K₂ [79]. In the case of the ^{39,41}K₂ isotope, the long-time spectrum reveals a regular dephasing of the wave packet and some fractional revivals around 38, 60 and 82 ps.

In the frequency domain both Fourier spectra depicted in Figure 5.3c and Figure 5.3d contain a group of frequencies around $\omega_0^{(1)} \approx 65 \text{ cm}^{-1}$. Other frequency groups are observed at $\omega_0^{(2)} \approx 130 \text{ cm}^{-1}$ and $\omega_0^{(3)} \approx 195 \text{ cm}^{-1}$. At $\omega_x \approx 90 \text{ cm}^{-1}$ an additional peak is observed, which is attributed to the population in the ground state [80].

The pump pulse excites the vibrational levels of the A¹Σ_u⁺ state in the ^{39,39}K₂ isotope around $v = 12$ ($v = 9 - 18$). The region where the most effective perturbation occurs is where the two vibrational levels of the A¹Σ_u⁺ state ($v = 12, 13$) are close [81, 82] to the vibrational levels of the b³Π_u state ($v = 23, 24$). This induces a shift of these perturbed vibrational levels of $+1.2 \text{ cm}^{-1}$ and $+2.1 \text{ cm}^{-1}$, respectively [76, 81]. The beat structure arises from the spectral hole existing in the frequency spectrum of the wave packet in the A¹Σ_u⁺ state (Figure 5.3c). For the ^{39,41}K₂ isotope no effective perturbation was found in the excitation range of the pump pulse. The vibrational levels contributing to the wave packet are perturbed to a very small amount and the energy transfer is smaller and slower (Figure 5.3d).

The described experimental results are in excellent agreement with the theoretical simulations [76, 80].

5.1.6 Femtosecond Pump–Probe Spectroscopy on Na₃

In this section the dependence of the vibrational dynamics of the Na₃ molecule on the shape of the pump pulse by means of femtosecond pump–probe spectroscopy is presented. The experiments reveal the possibility of influencing molecular processes by using shaped laser pulses.

The equilibrium geometry of a triatomic molecule is an equilateral triangle. A triatomic molecule has three vibrational degrees of freedom, which can be described in normal modes: Q_S (the symmetric stretch mode), Q_X (the symmetric bend mode) and Q_Y (the asymmetric stretch mode), as displayed in Figure 5.4 [83].

The superposition of the asymmetric stretch (Q_X) and the bending vibration (Q_Y) modes denotes a *pseudorotation* motion [84]. It can be time-resolved for example by transient two-photon ionization experiments. The situation of a triatomic molecule with its three modes is quite different from

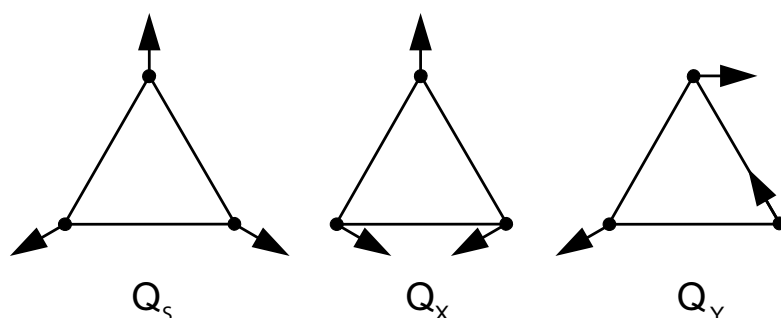


Figure 5.4: The normal modes of a triatomic cluster: the symmetric stretch mode (Q_S), the symmetric bending mode (Q_X) and the asymmetric stretch mode (Q_Y).

an isolated oscillating dimer, which vibrates in its single mode until eventually it radiates back to the electronic ground state or predissociates. The coupling of vibrational modes in a triatomic molecule (or a larger system) can be considered as the onset of *internal vibrational redistribution* (IVR). This was nicely demonstrated for Ag_3 [73].

The process of fragmentation becomes even more significant as the number of internal degrees of freedom inside the molecule increases.

The electronic $\text{B} \leftarrow \text{X}$ transition in Na_3 was investigated with transform-limited pulses of about 100 fs duration (at FWHM), whereby the pump and probe photons were centered at 620 nm (see Figure 5.5). The duration of both pump and probe pulses was 100 fs. The transient shows a pronounced molecular vibration, indicating only one vibrational mode of 320 fs duration, which corresponds to the symmetric stretch (Q_S) mode of Na_3 in the B-state [53,59]. There is, however, no indication for the asymmetric stretch, the bending mode or for pseudorotation. In this spectrum the strong modulation of the ion signal around $\Delta t = 0$ can be attributed to interferences between the pump and probe pulses. Furthermore the Na_3 transient is symmetric with respect to zero origin of time, due to the fact that at negative time delay the pump and probe pulses change their role.

The Influence of the Pulse Shape on the Na_3 Dynamics

The pump–probe experiment shown in Figure 5.5 is now performed by changing one single parameter: the linear chirp of the pump pulse.

The simplest way to change the linear chirp and thus the duration of a femtosecond pulse is to pass it through an optical arrangement of dispersive components. The setup in Figure 5.6 consists of two parallel gratings used to create linear downchirped pulses. In this case the shorter wavelengths travel

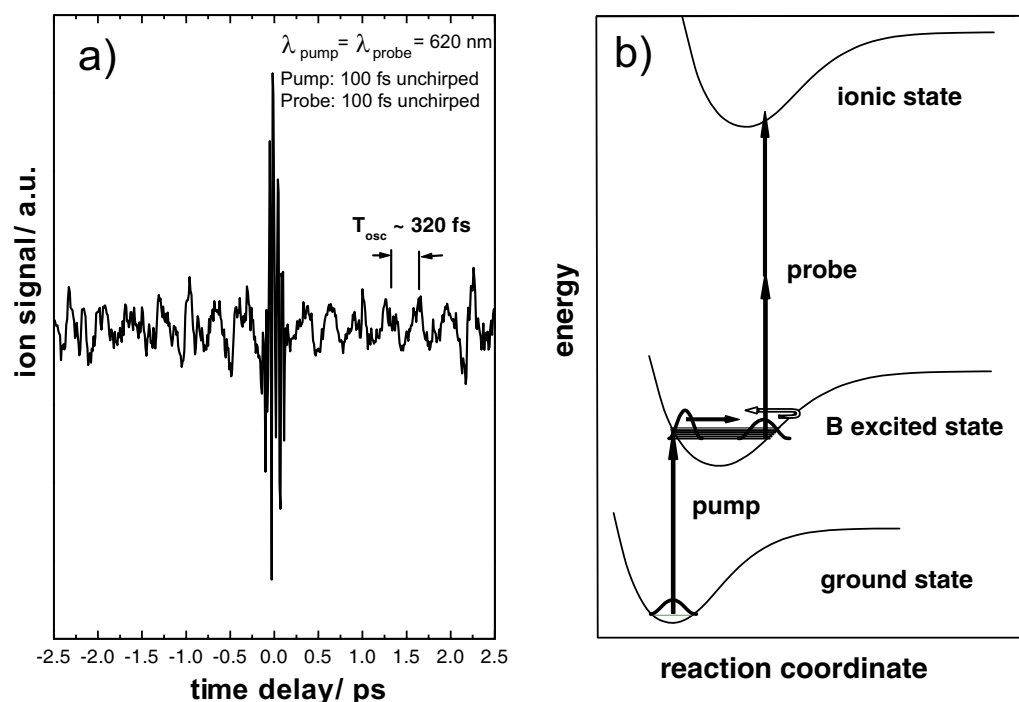


Figure 5.5: (a) Transient spectrum revealing wave packet dynamics of Na_3 on the B electronic excited state. The pump-probe signal recorded with pulses of 100 fs (FWHM) features an oscillatory behavior with a period of $T_{osc}^{\text{Na}_3} \sim 320$ fs corresponding to the symmetric stretch (Q_S) mode. (b) The principle of transient two-photon ionization. $\lambda_{pump} = \lambda_{probe} = 620$ nm (taken from Refs. [59, 75]).

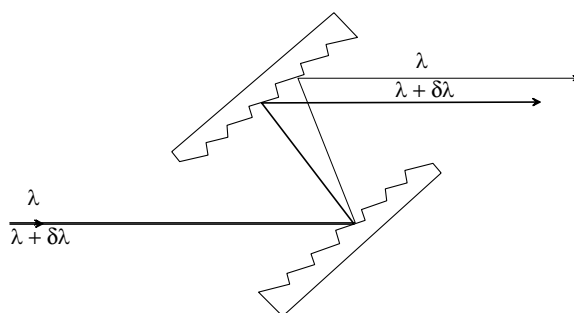


Figure 5.6: Grating arrangement to generate linearly chirped laser pulses.

faster than the longer wavelengths. The duration of the chirp pulse and its spectral sequence depends on the spatial separation between the gratings.

Figure 5.7a shows the corresponding Na_3 pump-probe spectrum, recorded with a 400 fs downchirped pump pulse (blue faster than red), whereas the

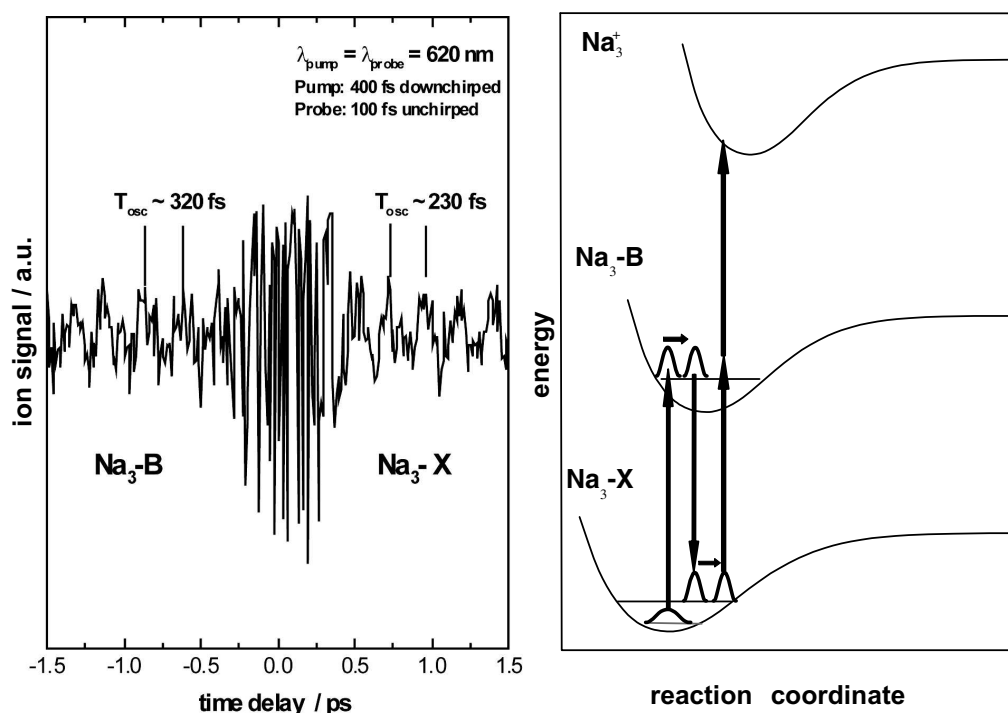


Figure 5.7: (a) Pump-probe spectrum of Na_3 obtained under identical experimental conditions as in Figure 5.5a, except that the employed pump pulse was linearly downchirped to a duration of 400 fs. The oscillation time of 230 fs corresponds to the symmetric stretch vibration of the electronic ground state of Na_3 . (b) Schematic view of the Stimulated Raman-pumping process: The blue part of the chirped pump pulse excites the cluster. Then the red components stimulate it back down to the electronic ground state, but Stokes-shifted to a higher vibrational level. The resulting wave packet dynamics is probed by the delayed probe pulse, which ionizes the cluster from the oscillating ground state. $\lambda_{\text{pump}} = \lambda_{\text{probe}} = 620 \text{ nm}$ (taken from Refs. [59, 75]).

duration of the probe pulse remains constant. Instead of the known oscillations in the B-state with a period of 320 fs, the Na_3 spectrum features oscillations of 230 fs period. This corresponds to the symmetric stretch mode of the electronic ground state of the Na_3 cluster [53]. The explanation is given in the scheme displayed in Figure 5.7b. The leading frequencies (shorter wavelengths) create a wave packet in the B-state of the Na_3 cluster, which propagates on the potential energy surfaces. It is then dumped down into the ground state (X-state) by the delayed longer wavelength components of the same (pump) pulse, like in a stimulated Raman pump process. The observed

oscillatory motion of the ground state is then monitored by the unchirped probe pulse via two-photon ionization. At negative time delays the vibrational period of 320 fs remains unchanged because in this temporal region the pump and probe pulses change their role. Here the observed dynamics occurs in the B electronic state of the Na_3 cluster, as expected.

This simple experiment indicates the dependence of the intramolecular dynamics on the irradiated pulse shape. Thus is it possible to influence molecular dynamics by modifying only the shape of the applied laser pulse.

5.2 Control of Molecular Reactions

This section presents briefly the theoretical schemes for controlling molecular reactions by employing laser light. These strategies were developed after the evolution of the experimental techniques for observing reaction dynamics in real time.

The temporal control scheme, also known as pump–dump or pump–control scheme is presented in section 5.2.1. This method advances from the pump–probe technique described in section 5.1.4 and uses the time delay between the two pulses as a reaction control parameter. The Brumer-Shapiro scheme, outlined in section 5.2.2 takes advantage of quantum mechanical interferences in order to selectively create the desired chemical products.

STIRAP (*Stimulated Raman scattering involving Adiabatic Passage*) is another control scheme of population transfer between specific quantum states of a molecular system. It was first proposed by K. Bergmann in 1990 [85]. Consider a three-state system, whereby each state is nondegenerate and there is no direct coupling between states $|1\rangle$ and $|3\rangle$. A pump pulse populates the intermediate state $|2\rangle$ starting from the initial state $|1\rangle$ and a so-called "Stokes" pulse couples the intermediate state to the final state $|3\rangle$. If the Stokes pulse precedes but overlaps the pump pulse 100 % efficient population transfer from state $|1\rangle$ to state $|3\rangle$ can be achieved [86,87].

Section 5.2.3 describes briefly the Optimal Control Theory, which is a more general method of the above mentioned control strategies. The procedure implies the finding of a laser pulse shape which optimally drives a reaction onto the desired path in order to obtain the desired selectivity. A further development of this theory is the feedback-control scheme [5], which is also used in this work. Hereby the optimal pulse is found by an optimization method which iteratively improves its properties in order to maximize/minimize a measurable signal representing the objective state. The optimization algorithm used in this work is based on evolution strategies which are presented in section 5.2.4.

5.2.1 Temporal Control: The Tannor-Rice Scheme

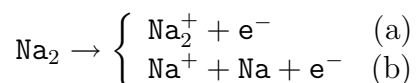
The Tannor-Rice method for selective control in a photo-induced reaction is based on the use of timing between sequential pulses of an applied electric field to guide the temporal evolution of a wave packet [88, 89].

Consider a triatomic molecule, ABC, with a stable configuration in its ground state (minimum) and two possible fragmentation channels on the ground state potential energy surface: AB + C and A + BC. The control problem reduces itself to find the time dependent electric field, which starting from the initial state (ground state, $v = 0$) sends the wave packet to the desired channel.

Generally, a wave packet prepared on an excited state by a short laser pulse is not in a stationary state. Thus its center moves along the excited state surface and its shape changes because of dephasing. At some time after the excitation, there will be more wave packet amplitude over the $ABC \rightarrow AB + C$ channel. A second ultrashort laser pulse is used to dump the wave packet from the excited state to the ground state, whereby mostly AB + C are formed. At some other time after excitation, there might be more amplitude over the $ABC \rightarrow A + BC$ channel; then the dump pulse will form predominantly A + BC products. Hence the selectivity in reaction product formation is achieved by the different transfer of wave packet amplitude into one of the two channels of the ground state. The scheme uses the Ehrenfest theorem by associating the wave packet dynamics with classical trajectories [90]. The time difference Δt between the two pulses is the time in which the wave packet propagates on the excited state potential surface and represents the "control knob". This method is also known as a *pump-dump control scheme*.

Verifications of the Tannor-Rice proposition are the experiments on XeI of the Zewail group [91] and on Na₂ of the Gerber group [92].

The first mentioned experiment showed that the product yields in the reaction $Xe + I_2 \rightarrow XeI + I$ can be modulated only by varying the delay time between two pump pulse excitations [91]. The first pulse creates a coherent wave packet on the B-potential surface of the reactant I₂. The wave packet oscillates with a well-defined frequency as the amplitude of I₂ motion changes. Then the second pump pulse is applied after a time delay corresponding to maximum separation of the Iodine atoms. It excites the wave packet above the threshold for reaction and forms XeI and I. The XeI product shows an oscillatory dependence on the time separation between the two pulses and reflects the wave packet motion of the I₂ reagent. The other experimental approach [92] used the competing pathways in the reaction



Hereby the autoionization reaction (a) and autoionization-induced photofragmentation reaction (b) were separated by varying the time delay between the two pulses, as well. Three photons resonantly generate Na_2^+ . The dimer is excited from the ground state to the $2\Pi_g$ state via the intermediate $A^1\Sigma_u^+$ state by the first pulse. Further excitation from the $2\Pi_g$ state produces Na_2^+ by direct excitation to the ground ionic state (a). The (b) process produces doubly excited neutral molecule Na_2^{**} which undergoes autoionization and autoionization induced fragmentation to generate Na^+ and Na . More details can be found in Ref. [93].

Although the Tannor-Rice method does not depend on the relative phase between the two pump and dump pulses, molecular dynamics can be influenced by controlling this relative phase. The experiment of the Fleming group [94] used two phase-locked pulses to control the population of I_2 in an excited state. The first pulse creates a wave packet in the B state of the iodine dimer. The second pulse generates a second wave packet which can interfere with the first one on the same excited state. Constructive or destructive interference patterns are observed depending not only on the time delay but also on the phase difference between the two pulses (phase-locking angles of 0° and 180° , respectively) as well as on the evolution of the first wave packet on the PES of the excited state. The experiment demonstrated that the population can be controlled by time-dependent phase-locked interferences.

The pump-dump control scheme is a most appropriate method for increasing the selectivity of a chemical reaction by employing specially designed laser pulses. In Ref. [88] the significance of optimal shaped pulses for the dump process was discussed. The optimal form of the dump-pulse was calculated as a convolution of the pump pulse with the molecular dynamics on the excited state.

5.2.2 Phase Control: The Brumer-Shapiro Scheme

A year after Tannor and Rice introduced their pulse timing control method, Brumer and Shapiro proposed another control scheme [95, 96] in which branching control of different products in a reaction can be influenced by three characteristics:

- The solutions of the Schrödinger equation depending on the energy describe the system completely. Then any solution of the time-dependent

Schrödinger equation can be represented as a superposition of the time-independent eigenstate solutions, associated with the dependence $e^{-iE_n t/\hbar}$ for each eigenstate $|n\rangle$ of energy E_n .

- Correlation between product specific wave functions and total system eigenfunctions is possible.
- If two independent pathways which connect the initial state with the final states are found in the system, and if the reaction probability is proportional to the square of the sum of the amplitudes (not simply the sum of transition probabilities) associated with individual transitions from the initial to the final state, a selective control of products in a specific final state can be achieved.

This scenario does not have to take into account the competition between processes like IVR and bond breaking, i.e. dynamics occurring on intermediate states. For example, the two independent pathways can be two different dissociative final states which can be resonantly excited by one or three photons (or 2 and 4 photons, respectively) of the same total energy: $E = 1 \cdot \hbar\omega_1 = 3 \cdot \hbar\omega_3$ (or $E = 2 \cdot \hbar\omega_2 = 4 \cdot \hbar\omega_4$). The two excitation pathways between the initial state and the two (degenerate) final states can interfere. By changing the relative phase between the two excitation sources ω_1 and ω_3 , constructive or destructive interferences between the two possible routes occur. This leads to a selectivity of the product formation because the control source (the relative phase) modulates the interference pattern of the product wave functions. The principle of this method is similar to a diffraction pattern observed in a double-slit experiment. Hereby, an oscillatory diffraction pattern originating from two waves which interfere after passing the two slits is measured.

Gordon and co-workers experimentally verified the idea of Brumer and Shapiro. The model systems used were HI and DI [97, 98] and H₂S [99]. The control objective was the branching photo-dissociation and photo-ionization of the aforementioned systems by interference between one-photon/three-photon transitions. After the DI dissociation, a Deuterium atom in its electronic ground state and an electronically excited I* atom are produced. The excited Iodine atom is detected by one-photon ionization. The ion signals of DI⁺ and I⁺ reveal a sinus dependence of the phase difference between the two monochromatic lasers. The constant phase lag of 150° between the two oscillations is responsible for the controlled concentration ratio of the two products. Details about the experiments can be found in Ref. [93].

5.2.3 Optimal Control

The presented control strategies are accurate if the molecular Hamiltonian and the PES are known over all nuclear separations. A precise calculation of bond angles, nuclear distances, vibrational frequencies, etc. is usually difficult. For example, the Brumer-Shapiro scheme faces the problem that the same intermediate state leads to different reaction products. In the Tannor-Rice method it is not possible to predict (or expect) that in the time when IVR is not yet relevant (at least for complex systems), the molecule reaches a particular configuration which allows the control of the desired process. A thought is worth considering whether it is possible to adapt the laser pulse to the molecular system to achieve the desired selectivity.

The first approach to find a laser pulse shape which influences a molecular process in order to control a chemical reaction product was the Optimal Control Theory (OCT). This theory was first developed by Rabitz and co-workers [100] and later by Kosloff et al. [101]. The latter one deals with a formalism in which it is possible to optimize the transfer of population into the desired exit channel by varying the characteristics of the applied laser field. The goal is to maximize the functional of the laser field J [93]:

$$J = \langle \psi(t) | \hat{P}_{i,f} | \psi(t) \rangle \quad (5.10)$$

at some time $\tau = t$. Here the indexes i and f suggest the initial and the final state, respectively.

The theoretical pulse shape is generated in the laboratory and applied on the molecular system (**open loop**). The task of the OCT is to find a laser field which causes an effective population transfer to the selected target channel while suppressing the unwanted product channels, e.g. by creating constructive interferences in the desired reaction product and destructive interferences in any of the unwanted states along the chosen pathway towards the reaction goal [6]. Thus a successful control is achieved if the shaped laser field *cooperates* with the molecule dynamical processes. In principle, fragmentation is always possible if the electronic excited state potential allows the exit of the propagating wave packet. This occurs under the condition that the wave packet leaks out before intramolecular dissipation processes or before a collision with a neighboring molecule takes place [102]. Photoisomerization processes can be controlled with the help of OCT as well [103–105].

The objective functional J has to maximize the transition probability from the initial state i to the final state f while minimizing the laser energy [106]:

$$\begin{aligned}
J_{i,f}(\epsilon(t)) = & |\langle \psi_i(\tau) | \phi_f(\tau) \rangle|^2 - \alpha_0 \int_0^\tau [\epsilon(t)]^2 dt - \\
& - 2\text{Re} \left[\langle \psi_i(\tau) | \phi_f(\tau) \rangle \cdot \int_0^\tau \langle \psi_f(\tau) | \frac{\partial}{\partial t} + i[H_0 + V - \mu\epsilon(t)] | \psi_i(t) \rangle dt \right].
\end{aligned}
\tag{5.11}$$

In the expression (5.11) $\psi_i(t)$ is the wave function driven by the optimal laser field $\epsilon(t)$, the initial wave function is $\psi_i(0)$ and the final state $\phi_f(\tau)$ is the target state at the final time τ . $\psi_f(t)$ is a Lagrange multiplier which is introduced to assure the satisfaction of the Schrödinger equation. H_0 is the kinetic energy operator, V is the potential energy and μ is the transition dipole moment. J is optimized with respect to the molecular wave function ψ_i , to the Lagrange multiplier $\psi_f(t)$ and to the electric field $\epsilon(t)$. One gets three coupled differential equations which have to be solved iteratively. Thus after each generation a new electric field is obtained which increases J until self consistency is reached.

The shaped laser pulses, i.e. the amplitude and phase of the electric field, can be then calculated so that a maximum overlap of the propagating wave function with the selected target state is achieved at the end of the interaction time. In the laboratory they can be translated on pulse shaping devices (see Chapter 3). Finding this so-called *optimal laser field* is however not trivial, since, as mentioned before, the approximations made in the theoretical efforts do not always correspond to the real world. For polyatomic molecules there is an amount of uncertainty in the Hamiltonians (the third term in the right part of equation (5.11)) and developing OCT for these systems is a challenging task. In his pioneering work, Rabitz formulated an optimal control problem for the time-dependent Schrödinger equation [100]. Later on the concept of feedback loop was introduced, whereby the electric field of the femtosecond laser pulse is adapted to the specific molecular system in order to drive the chemical reaction to the desired end product in an iterative scheme [5]. The loop is now **closed**, by using a computer in which a learning algorithm is implemented:

Over a series of pulses the algorithm learns an optimal sequence. The experimental apparatus, which consists of a laser, a sample of molecules, and a measurement device, acts as an analog computer that solves Schrödinger equation exactly, in real-time.
(Quote from Ref. [5])

The learning algorithm¹ is inspired from nature's ability to adapt itself to a

¹Simulated Annealing, Evolution Strategies and Genetic Algorithms are widely used for their non-deterministic character.

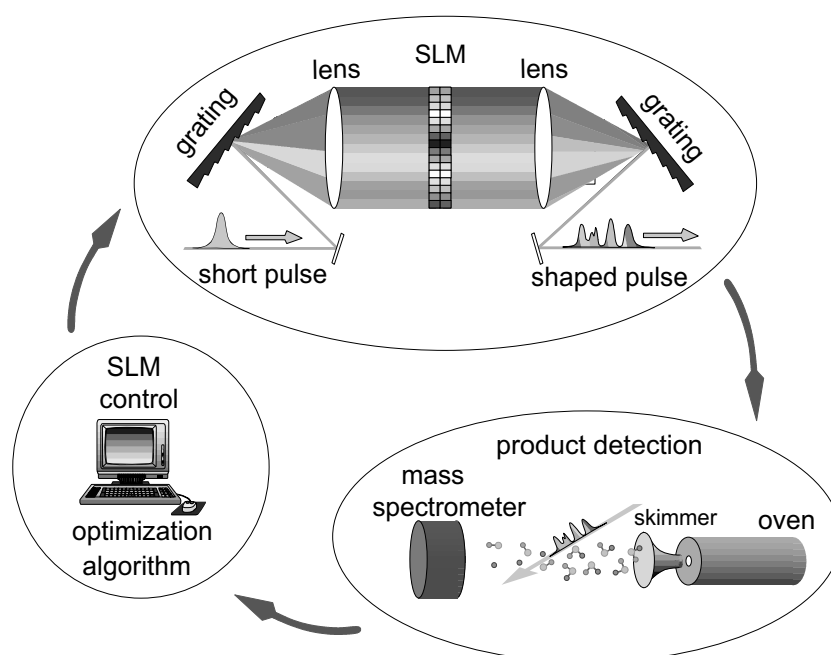


Figure 5.8: Experimental realization of the feedback loop. SLM stands for Spatial Light Modulator (the liquid crystal based pulse shaper). The optimization algorithm writes patterns onto the liquid crystal window, which are sent to the neutral molecular beam. The shaped pulses are evaluated by the ion signal they produce. The iterative procedure changes the shape of the laser field in order to maximize/minimize the ion yield. After convergence the optimal pulse is found.

new environment. In this work an optimization algorithm based on evolution strategies is applied (see section 5.2.4).

The goal of the optimization is to let the pulse shape solve the time-dependent Schrödinger equation. The adaptive feedback-control scheme iteratively modifies the laser pulse until the experimental observable (representing the desired target state) is maximized or minimized. This is done by *feeding* the pulse shaper with information about the measured signal so that the electric field pattern is modified until the response signal does not significantly change (convergence is achieved). In our laboratory the measured signal is the photo-ion current (or ion signal ratio). This represents the feedback signal used by the optimization algorithm. The pulse forms written by the optimization algorithm onto the pulse shaper are weighted by their ability (*fitness*) to increase/decrease the ion signal. Depending on their fitness, only the pulses which produced the highest ion signal (*best individuals*) are selected and used to create other pulse forms (*children*) in the next iteration.

In this way the algorithm learns the optimal sequence for the investigated system, i.e. the best pulse for a desired process in a particular molecule. All of this is achieved without an *a priori* knowledge of the molecular Hamiltonian and thus of the PES during the optimal path towards the selected target state. Figure 5.8 illustrates the closed loop experiment implemented in our laboratory.

Many groups applied the feedback-informed loop scheme in the laboratory. Processes, like fluorescence efficiency in organic dyes [107], fragmentation of organometallic molecules [108], ionization [109], impulsive stimulated Raman scattering (ISRS) [110], and high harmonic generation [111] were objectives of the optimization.

The possibility of controlling chemical processes opened a fascinating door to physical chemistry, but one of the most interesting topics is the control process itself. The problem of inversion introduced by Rabitz [6] refers to the information encoded in the optimal pulse. Specific molecular "data" (the shape of the PES and/or indication of the wave packet's vibrational period within the subpulse spacings) can be extracted out of the optimized laser field. For complex systems this information can be very well hidden, so that supplementary analysis (theoretical calculations, pump-probe spectroscopy) is necessary until the optimal pulse is understood (see Chapter 6, section 6.3.4). The main goal of this work is to present a few cases where optimal pulses can be deciphered.

5.2.4 Evolution Strategies

The evolution strategies (ES) have been first introduced in Berlin by I. Rechenberg [112] and further investigated by H. Schwefel [113].

Their advantage is that they converge under the given experimental conditions, they deal with experimental noise [114] and maybe the most important is their global seek strategy. In this way, in a fairly large searching space, ES are able to find a qualitatively acceptable solution.

The codes implemented in ES are real values. One individuum is represented by a vector N of real numbers (*genes*). N is also known as the number of parameters to be optimized. The initial population contains μ individuals. From these individuals one randomly chooses *pairs* which will generate children. There are three important operators: *cross-over*, *mutation* and *survival of the fittest*. These operators will act as following:

- **Cross-over:** the two pairs are recombined by randomly changing their genes. Afterwards, either the two recombined individuals will be carried along or one individuum will be randomly selected and deleted. Another cross-over

method is to add the genes of other pairs and to inscribe the resulting average value as gene of a new individual. The cross-over is responsible in the ES for the generation of an offspring in the population. Moreover, the cross-over operator avoids early convergence in local minima.

- The **mutation** operator acts on the offspring of the pairs. A random number $n(\sigma)$ is added or subtracted from each gene. These random numbers are normally distributed around zero (in a Gauss distribution) with σ at FWHM, also called *mutation increment*. σ plays a very important role in the global convergence of the algorithm. The mutations are responsible for the (new) search strategies and convergence. Hence, the mutation increment σ has to be adapted during the optimization process. There are two methods in which σ can be adapted: *self-adaption* and the $\frac{1}{5}$ *rule*.

a) *Self-adaption*. Here the mutation increment itself is subject to optimization. This method is also known as *self-optimization*.

b) The $\frac{1}{5}$ *rule* is a rule of thumb in adapting the mutation increment to the mutation's success in one generation. If the mutation's success is larger than 0.2 than σ will be increased. If the mutation's success is smaller than 0.2, the mutation increment has to be diminished. One could say that the algorithm *opens its eyes*: if the mutation is successful the algorithm has found the right path in the searching space. Thus it has to be helped in finding the global solution by increasing the mutation increment σ . On the contrary, if the mutation is less successful, it means that the algorithm is not on the right track and has to search the solution in small steps. In this manner, one increases the probability of success and avoids trapping in local minima. In this work σ is increased by a factor of 1.3 in the case of success and diminished by a factor of 0.8 in case of failure.

- In the next step, all individuals have to be evaluated based on their qualities. The **evaluation** of the individuals occurs after comparison with a goal function. The smaller the difference between the *present* individuals and the *desired* population, the better the evaluation. In our experiments, the evaluation operator takes the desired ion signal intensity into account and reports the mutated individuals to it.

- The last step in the ES is the selection, or **survival of the fittest**. The selected individuals will be parent individuals in the next generation. They have the highest evaluation, or the best *fitness*. In our experiments they are the pulse forms which produce the highest ion signal. The other individuals with lower fitness are deleted.

Figure 5.9 illustrates the course of the optimization algorithm. Briefly, the ES creates an initial population of 10 individuals (μ individuals). Each

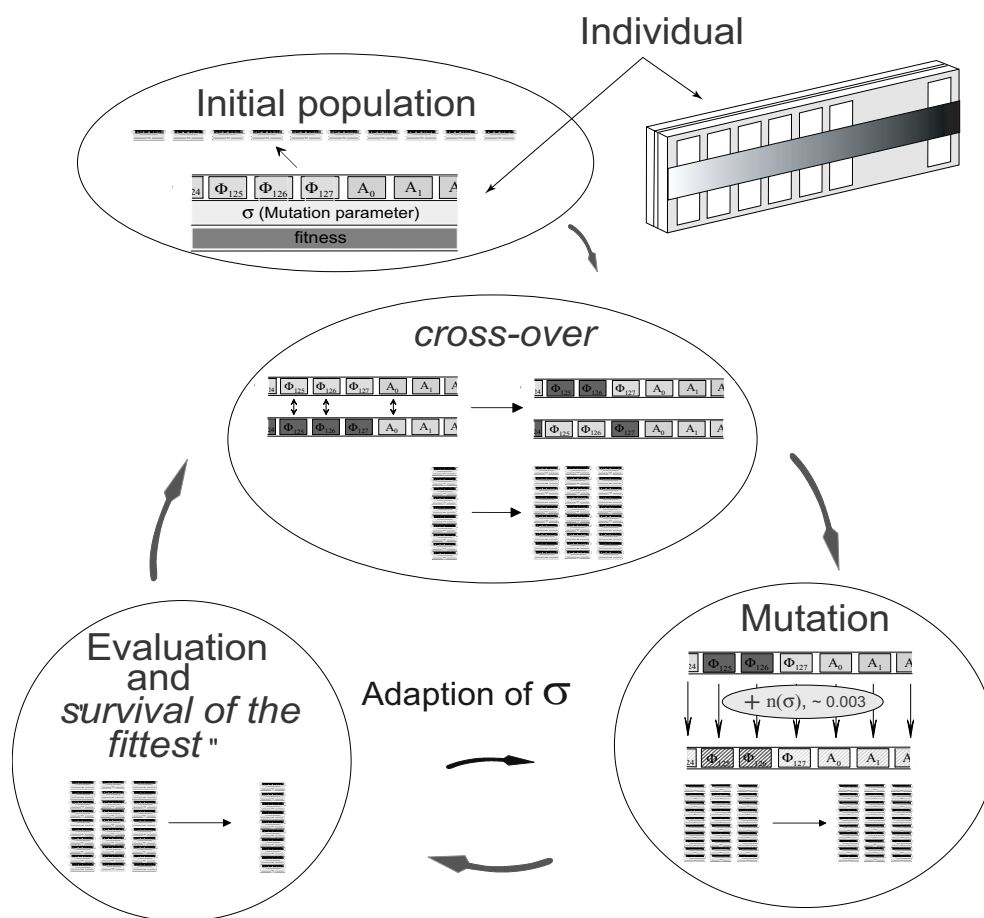


Figure 5.9: Principle of feedback optimization with evolution strategies. An initial population of 10 individuals (10 pulse forms) is created corresponding to 10 different patterns of the 128 phase and/or 128 amplitude values of the laser field. The individuals are recombined, mutated and then written on the modulator mask. The experimental observable (e.g. ion signal) determines the quality (*fitness*) of each individual. Only the best 10 pulse forms are selected from the old generation as parents in the new generation.

of these individuals represents an array of 128 or 256 values corresponding to the phase or phase and amplitude values written on the liquid crystal mask. Thus each individual is an entity corresponding to a complete setting of the liquid crystal mask and generates a particular pulse form. All individuals in the initial population are randomly chosen. From these 10, two of them are randomly picked with equal probability and recombined by the cross-over operator independent of their fitness. This is repeated 15 times whereby a pop-

ulation of 30 individuals is created. The mutation operator slightly changes all 30 individual values with a parameter σ (starting value of 0.003) which represents the FWHM of a Gaussian distribution of random numbers. The individuals are translated into drive voltages on the modulator mask. There is a 200 ms waiting time given to the liquid crystal molecules to complete their rotation. The 30 pulse forms are focused onto the supersonic jet, whereby the molecules are fragmented/ionized. Each pulse produces a certain amount of ions. The current intensity (or ratio between two species) describes the fitness of each individual. Based on their fitness the 30 individuals are evaluated. Depending on the optimization goal (maximization/minimization) only 10 individuals which produced the highest/lowest ion signal (or ion signal ratio) are selected as parents for the next iteration. Variations of these particular numbers is certainly possible; they were chosen after few experimental trials as a trade-off between a fast convergence and large population.

A *free optimization* is an experiment where all 128 phase or amplitude values (256 values for phase and amplitude) are creating the searching space of the algorithm. In this way one takes advantage of the full capability of the pulse shaper. The searching space can be also reduced in order to achieve a faster convergence. Only a class of solutions is allowed and the optimum is searched in this reduced space. This is also known as *parametric optimization* (or *parametrization*). The result depends on the class of solutions (e.g. subpulse timings, pulse intensity, spectral FWHM, zero-order phase, linear, quadratic or third order chirp, etc.). Theoretical and experimental investigations on parametric optimization are described in Refs. [115–118]. More information about ES implemented in our experiment can be found in [20, 40].